Nature **401,** 811–815; 1999

The Toll-like receptor 2 is recruited to macrophage phagosomes and discriminates between pathogens

David M. Underhill*, Adrian Ozinsky*, Adeline M. Hajjar, Anne Stevens, Christopher B. Wilson, Michael Bassetti & Alan Aderem

Department of Immunology, University of Washington, H-574 Health Sciences, Box 357650, Seattle, Washington 98195, USA
** These authors contributed equally to this work*

Macrophages orchestrate innate immunity by phagocytosing pathogens and coordinating inflammatory responses[1]. Effective defence requires the host to discriminate between different pathogens. The specificity of innate immune recognition in *Drosophila* is mediated by the Toll family of receptors[2,3]; Toll mediates anti-fungal responses, whereas 18-wheeler mediates anti-bacterial defence[4–6]. A large number of Toll homologues have been identified in mammals, and Toll-like receptor 4 is critical in responses to Gram-negative bacteria[7–11]. Here we show that Toll-like receptor 2 is recruited specifically to macrophage phagosomes containing yeast, and that a point mutation in the receptor abrogates inflammatory responses to yeast and Gram-positive bacteria, but not to Gram-negative bacteria. Thus, during the phagocytosis of pathogens, two classes of innate immune receptors cooperate to mediate host defence: phagocytic receptors, such as the mannose receptor, signal particle internalization, and the Toll-like receptors sample the contents of the vacuole and trigger an inflammatory response appropriate to defence against the specific organism.

Macrophage phagocytosis of the yeast cell-wall particle zymosan is accompanied by secretion of the inflammatory mediator tumour necrosis factor-α (TNF-α). Internalization of zymosan is mediated, in part, by the mannose receptor, a classic example of an innate immune pattern-recognition molecule, but the signalling pathway that elicits TNF-α production is unknown[12]. Given the role of Toll-like receptors in pro-inflammatory signalling during innate defence, we explored whether these molecules are also found on phagosomes. We expressed haemagglutin A (HA)-tagged murine Toll-like receptor 2 (TLR2) in the mouse macrophage cell line, RAW-TT10. In the absence of a phagocytic stimulus, the receptor was distributed uniformly on the cell surface (Fig. 1a). After a 5-min incubation with zymosan particles, TLR2 was highly enriched on phagosomes (Fig. 1b, c). Phagocytosis occurs through a series of discrete steps: initially the particle is bound to the cell surface; actin polymerization leads to pseudopod extension around the particle; the particle is completely engulfed by the cell; and lastly actin is depolymerized, allowing further phagosome maturation through membrane-transport events[1]. The enrichment of TLR2 was apparent throughout all phases of internalization (Fig. 1b, c, zymosan particles 1–4): the receptor was enriched under bound particles (zymosan 1), in processes extending around extracellular particles (zymosan 2) and in membranes around fully engulfed particles (zymosan 3), and it remained enriched on the phagosome for several minutes after actin disassembly (zymosan 4; and data not shown). Within 10 min after internalization, however, TLR2 was no longer enriched on the vacuole (data not shown).

Phagocytosis of particles is tightly coupled to the production of pro-inflammatory cytokines, but the mechanism by which this occurs is unknown. The presence of TLR2 on phagosomes indicated that it might mediate pro-inflammatory signals during zymosan phagocytosis. To establish a role for TLR2 in zymosan-induced cytokine release, we needed to define a dominant-negative form of this receptor. Genetic evidence in the C3H/HeJ mouse indicates that a P712H substitution in the related Toll-like receptor 4 (TLR4) may act as a dominant-negative mutation of the receptor and prevent LPS signalling in the mouse[10,11,13]. We therefore constructed a putative dominant-negative mutant TLR2, in which proline 681 was replaced by a histidine (TLR2-P681H), a mutation that is equivalent to the P712H substitution in TLR4. Chinese hamsters fail to express functional TLR2 because of a frame-shift mutation in the receptor[14], making Chinese hamster ovary (CHO) cells an ideal model system in which to define dominant-negative mutants of TLR2 signalling. Expression of TLR2 in CHO cells resulted in a moderate level of constitutive activation of NF-κB, which was not increased substantially upon exposure of the cells to zymosan (Fig. 2a). CD14 has been shown to facilitate the activation of TLR2 by bacterial products[15,16]. Cotransfection of CHO cells with CD14 and TLR2 greatly enhanced zymosan-induced NF-κB activation (Fig. 2a), whereas expression of CD14 by itself did not mediate zymosan-induced signalling (data not shown). TLR2-P681H did not mediate zymosan-induced activation of NF-κB in the presence of CD14, indicating that the mutation abrogated the capacity of the receptor to signal (Fig. 2a). Importantly, TLR2-P681H acted as a dominant-negative inhibitor of TLR2-mediated activation of NF-κB (Fig. 2a). Identical results were obtained with *Staphyloccus aureus* (data not shown). When expressed in RAW-TT10 macro-

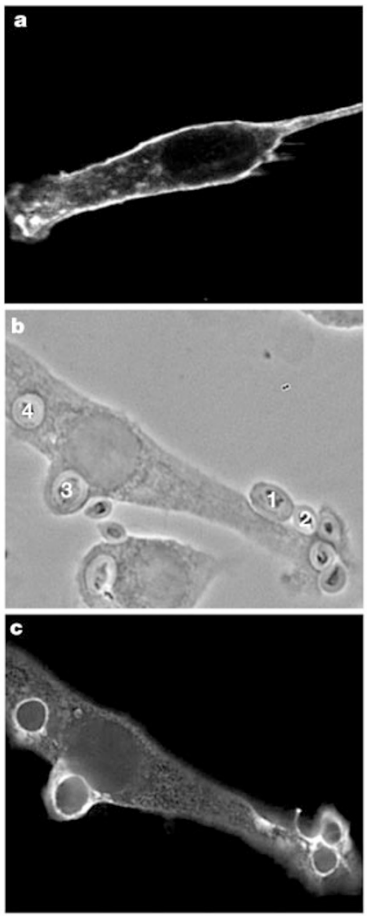

Figure 1 TLR2 is enriched on phagosomes containing yeast particles. **a**, Epitope-tagged TLR2 was detected on the cell surface by immunofluorescence microscopy in RAW-TT10 cells transiently expressing the receptor. **b**, When these cells were incubated with zymosan for 5 min and processed for immunofluorescence microscopy, zymosan particles, both external (particles 1 and 2) and internal (particles 3 and 4), were clearly visible by phase microscopy. **c**, TLR2 was markedly enriched around the particles during all stages of internalization.

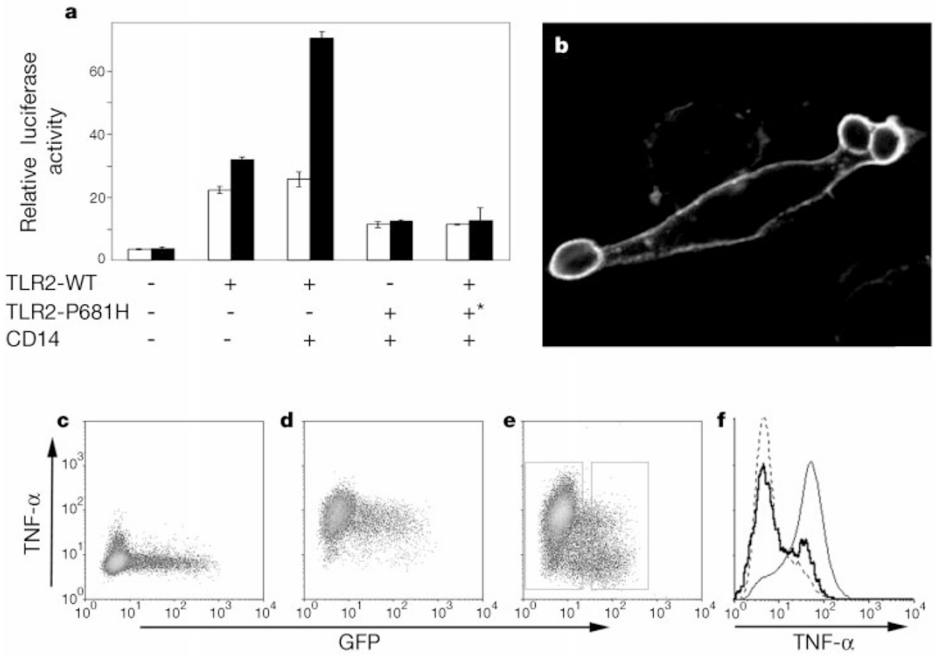

Figure 2 Expression of TLR2-P681H blocks zymosan-induced TNF-α production. **a**, The relative activity of a NF-κB-luciferase reporter was assessed in CHO cells transiently expressing the indicated constructs before (open bars) or after (filled bars) stimulation with zymosan. In the sample showing inhibition of TLR2 by TLR2-P681H (asterisk), the mutant receptor was cotransfected with the wild-type receptor at a 10:1 ratio. **b**, Epitope-tagged TLR2-P681H, transiently expressed in RAW-TT10 cells, was highly enriched on zymosan phagosomes. The HA tag was detected by immunofluorescence microscopy as in Fig. 1. **c**, **d**, RAW-TT10 cells transiently transfected with the control expression vector (pTIGZ2+) were stained for production of TNF-α and analysed by flow cytometry following no stimulation (**c**), or after incubation with zymosan (**d**). **e**, Cells expressing TLR2-P681H failed to induce TNF-α after stimulation with zymosan. **f**, Using the regions defined in **e**, the thin line indicates TNF-α produced in stimulated GFP-low cells, and the bold line indicates TNF-α produced in stimulated, TLR2-P681H-expressing cells (GFP-high). The dotted line indicates background, unstimulated TNF-α production; *y* axis, relative cell number.

phages, TLR2-P681H was distributed at the cell surface and was substantially enriched around zymosan-containing phagosomes, indicating that it was properly localized to function as a dominant-negative inhibitor of particle-induced signalling through endogenous TLR2 (Fig. 2b).

To determine whether TLR2-P681H was capable of inhibiting the production of pro-inflammatory cytokines during phagocytosis in macrophages, we designed a single-cell assay in which we could simultaneously analyse the expression of the mutant receptor and zymosan-induced TNF-α production. In this assay, transient expression of TLR2-P681H and green fluorescent protein (GFP) from a single bicistronic transcript permitted GFP intensity (as measured by flow cytometry) to reflect accurately the level of TLR2-P681H expression (see Supplementary Information). RAW-TT10 cells were transfected with a control vector expressing only GFP, and 100,000 cells were analysed by flow cytometry. TNF-α production remained at background levels over three logs of expression of GFP (Fig. 2c). When stimulated with zymosan particles, TNF-α production was induced equally in all cells irrespective of their level of GFP expression (Fig. 2d). Expression of TLR2-P681H correlated in a dose-dependent manner with the inhibition of TNF-α production induced by zymosan (Fig. 2e). Cells producing TLR2-P681H (as measured by GFP expression) clearly failed to produce TNF-α, whereas cells in the same sample that did not express the inhibitory receptor produced TNF-α. Expression of TLR2-P681H in RAW-TT10 cells also inhibited zymosan-induced activation of NF-κB, as measured by its translocation from the cytosol to the nucleus (see Supplementary Information). Particle binding and internalization were unaffected by the expression of the mutant receptor (data not shown; and see below), indicating that phagocytosis and particle-induced cytokine production were uncoupled in these cells. The full spectrum of TNF-α production by GFP-positive or GFP-negative cells (Fig. 2e, boxed regions) is shown in Fig. 2f. GFP-negative cells (Fig. 2f, thin line) had appreciable zymosan-induced TNF-α production, which was inhibited in TLR2-P681H-expressing cells (thick line), effectively to unstimulated levels (dotted line). Thus, TLR2 couples the phagocytosis of zymosan to TNF-α production, and the extent of the inhibition (>90%) suggests that this is the primary pathway.

As phagocytosis of yeast resulted in TLR2-mediated signalling, we examined the potential for this receptor to signal TNF-α production during the phagocytosis of other pathogens. TNF-α production induced during the phagocytosis of *S. aureus*, a Gram-positive bacterium, was completely inhibited by the expression of TLR2-P681H (Fig. 3), as was TNF-α induction by the Gram-positive bacterial cell-wall components lipoteichoic acid and peptidoglycan (data not shown). By contrast, TNF-α production elicited during the phagocytosis of *Salmonella minnesota R595*, a Gram-negative bacterium, was unaffected by the expression of TLR2-P681H (Fig. 3). Similarly, lipopolysaccharide (LPS), a key pro-inflammatory component of the Gram-negative bacterial cell wall, induced TNF-α normally in the presence of TLR2-P681H (Fig. 3). Thus, TLR2 discriminates yeast and Gram-positive bacteria from Gram-negative bacteria. The C3H/HeJ mouse, which bears a P712H mutation in TLR4, is hyporesponsive to LPS, indicating that TLR4 participates in the recognition of Gram-negative bacteria[10,11]. Expression of TLR4-P712H in RAW-TT10 macrophages strongly inhibited LPS-induced TNF-α production, whereas it had no effect on *S.-aureus*-induced signalling (Fig. 3). TLR4-P712H inhibited *S.-minnesota*-induced TNF-α production to a lesser degree than was observed with soluble LPS (Fig. 3). These data show that individual Toll family receptors convey specificity in mediating pro-inflammatory signals from different pathogens.

Further insight into the mechanism by which TLR2 signals was obtained by the observation that expression of the wild-type receptor partially inhibited zymosan- and *S.-aureus*-induced

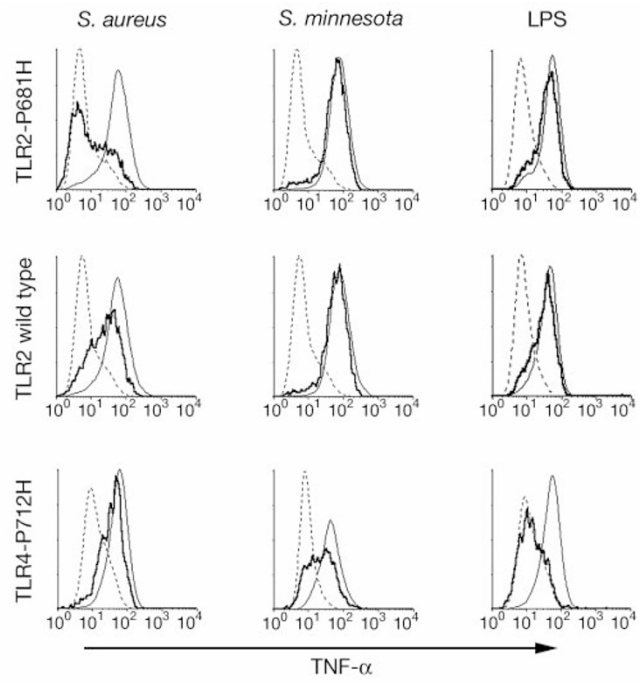

Figure 3 Inhibition of particle-induced TNF-α production by TLR2-P681H is selective. RAW-TT10 cells transiently transfected with TLR2-P681H (upper panels), wild-type TLR2 (middle panels) or TLR4-P712H (lower panels) were analysed for particle-induced TNF-α production. The cells were stimulated as indicated with *S. aureus*, *S. minnesota* or LPS. Using the regions defined in Fig. 2e, the thin lines indicate TNF-α produced in stimulated, GFP-low cells, and the bold lines indicate TNF-α produced in stimulated, TLR-expressing cells (GFP-high). The dotted lines indicate background, unstimulated TNF-α production; *y* axes, relative cell number.

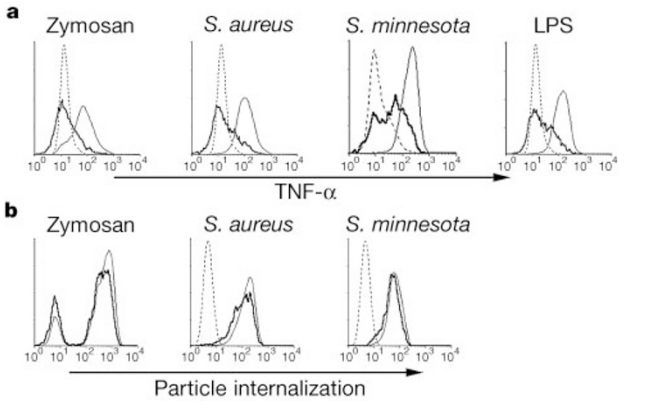

Figure 4 Expression of MyD88-DN blocks particle-induced TNF-α production but not particle internalization. **a**, RAW-TT10 cells transiently expressing MyD88-DN were stimulated as indicated with zymosan, *S. aureus*, *S. minnesota* or LPS, and TNF-α production was measured. Using the regions as defined in Fig. 2e, the thin lines indicate TNF-α produced in stimulated, GFP-low cells, and the bold lines indicate TNF-α produced in stimulated, MyD88-DN-expressing cells (GFP-high). The dotted lines indicate background, unstimulated TNF-α production. **b**, Cells transiently expressing MyD88-DN were incubated with fluorescently labelled zymosan, *S. aureus*, or *S. minnesota* as indicated, and particle internalization was assessed by flow cytometry; *y* axes, relative cell number.

TNF-α production, but had no effect on *S. minnesota*- and LPS-induced TNF-α production (Fig. 3; and data not shown). The data indicate that over-expression of the wild-type receptor may dilute out other molecules required for TLR2 function, perhaps a structural component of the receptor, and further shows that TLR2 does not participate in the response of macrophages to Gram-negative bacteria.

MyD88 is a cytoplasmic adaptor protein that binds to the Toll-homology domain of TLR4 and the interleukin-1 receptor (IL-1R), and mediates their downstream signalling[17–20]. Binding of MyD88 to these receptors is mediated by a C-terminal Toll-homology domain, whereas its N-terminal death domain is important for the propagation of the signal through the protein kinase IRAK (IL-1 receptor associated kinase). The C-terminal Toll domain of MyD88 is a dominant-negative inhibitor of TLR4 and IL-1R signalling, whereas the death domain constitutively activates these pathways[17–19]. Expression of the C-terminal MyD88 dominant negative (MyD88-DN) correlated precisely with inhibition of TNF-α production induced during the phagocytosis of zymosan and the Gram-positive bacterium, *S. aureus* (Fig. 4a). The failure of TNF-α induction could not be attributed to an inhibition of particle binding or internalization, as the internalization of fluorescently labelled zymosan, *S. aureus* and *S. minnesota* was unaffected by MyD88-DN expression (Fig. 4b). Thus, MyD88 is required for TLR2 signalling in the macrophage. MyD88-DN also inhibited TNF-α production induced by the Gram-negative bacterium *S. minnesota* and by LPS (Fig. 4a), although the inhibitor was less effective against the whole bacterium (as observed with TLR4-P712H in Fig. 3). These later data indicate that, during phagocytosis of Gram-negative bacteria, a MyD88-dependent pathway (presumably initiated by TLR4) and a MyD88-independent pathway may contribute to the complete induction of TNF-α. This hypothesis concurs with the observation that, although the TLR4 mutation in the C3H/HeJ mouse blocks soluble LPS signalling, Gram-negative bacteria still stimulate cytokine production (perhaps through Toll-independent pathways)[21]. Thus, both genetic data and our results indicate that TLR4 may be the primary mediator of LPS signalling, whereas our data show that TLR2 principally mediates signals from yeast and Gram-positive bacteria in macrophages. Previously, human TLR2 has been implicated in LPS signalling in non-macrophage cell lines, and it not clear why our data, obtained in cells that are naturally LPS-responsive, differ[22,23]; however, our data concur with genetic evidence in mice and hamsters, in which a mutation in TLR4 abrogates LPS signalling whereas a mutation in TLR2 does not[10,11,14]. We have also shown that the natural mutation in the TLR4 gene in the C3H/HeJ LPS-hyporesponsive mouse (P712H) acts as a dominant-negative inhibitor of TLR4 function. Notably, the corresponding proline-to-histidine mutation in TLR2 (P681H) also acts as a dominant-negative mutation in TLR2. This proline is conserved in all known mammalian Toll receptors, except TLR3 (ref. 7–9), and might couple Toll receptors to a common signalling pathway.

Macrophages are capable of detecting the nature of the pathogen within the phagocytic vacuole, but the mechanisms by which this occurs are unknown[1]. Our data indicate that the toll-like receptors may be recruited to phagosomes, where they sample the contents and determine the nature of the pathogen; TLR2 detects Gram-positive bacteria and fungi, whereas TLR4 detects Gram-negative bacteria. Thus, specific Toll-like receptors may distinguish the contents of the phagosome and participate in the elaboration of an inflammatory response appropriate for defence against a specific pathogen. □

Methods

Murine TLR2 cloning

Two mouse ESTs (Genbank AA863729 and D77677) with homology to the human TLR2 sequence were identified, and a 0.9-kilobase (kb) complementary DNA was generated by reverse transcription of RAW 264.7 total RNA using a primer spanning the stop codon in

the first EST (5′-GGTGGAGAACCTAGGACTTTATTGC-3′). Polymerase chain reaction (PCR) was carried out with the same primer, and the 5′ most homologous sequences in the second EST (5′-GCTCTATATTTCCAGAAATAAGCTG-3′). To obtain the complete open reading frame (ORF), 5′ rapid amplification of complementary DNA ends (RACE) was performed on RAW 264.7 RNA (Gibco-BRL). Products from 0.5 to 1.5 kb were amplified, cloned and sequenced, completing the murine TLR2 ORF (Genbank AF185284).

DNA expression vectors

The mammalian expression vector, pNeo/Tak, was constructed to combine expression of the tetracycline transactivator[24] from a tetracycline-regulated promoter (pTet-Tak, Gibco-BRL) with neomycin selection. The neomycin resistance marker was from pcDNA3 (Invitrogen), and the remainder of the plasmid backbone was derived from pBluescript SK (Stratagene).

The expression vector pTIGZ2+ was assembled to direct tetracycline-regulated expression of a protein from the same messenger RNA transcript as GFP. In this vector, the tetracycline-regulated promoter from pTetSplice (Gibco-BRL) directed expression of a mRNA encoding the protein of interest followed by the cap-independent translational enhancer region of pCITE (Novagen) driving translation of enhanced GFP (from peGFP-N1, Clonetech). The polyadenylation signal and remainder of the vector backbone were from pcDNA3.1/Zeo (Invitrogen). During construction, the tetracycline-inducible promoter was modified to contain two binding sites for the tetracycline transactivator instead of seven.

The HA-TLR2 expression vector was constructed by amplifying the coding region of mouse TLR2 from amino acids R21–S784 (removing the endogenous signal peptide) by PCR, and cloning the fragment into a modified pDisplay (Invitrogen) which provides a signal peptide and a haemagglutinin A epitope. pDisplay had been modified by deletion of the PDGF transmembrane domain and replacement of the neomycin resistance cassette by one with zeocin resistance (pcDNA3.1/Zeo, Invitrogen). For single-cell TNF-α measurements, the HA-tagged TLR2 coding region was transferred from pDisplay to TIGZ2+. The TLR2 dominant-negative P681H mutation was generated by PCR and confirmed by sequencing. The MyD88 dominant-negative construct was generated by amplifying the MyD88 C-terminal coding region (amino acids 146–296) by PCR from cDNA of RAW 264.7 cells and cloning the fragment into TIGZ2+. The murine TLR4 coding region was amplified by RT-PCR from RAW cells (Genbank AF185285), and cloned into pTIGZ2+. The dominant-negative P712H mutation was generated by PCR and confirmed by sequencing, and the resulting coding region was cloned into pTIGZ2+. Murine CD14 was amplified by RT-PCR from RAW cells and cloned into the expression vector pcDNA3.1/Zeo (Invitrogen).

Transfection

RAW 264.7 (ATCC# TIB-71) and CHO-K1 (ATCC# CRL-9618) cells were transfected as described[25]. All experiments were performed 24 h after transfection. For generation of a tetracycline transactivator-expressing RAW cell line, RAW 264.7 cells were transfected with pNeo/Tak, and stable cell lines were selected using 400 μg ml^{-1} G418 (Gibco-BRL). After 10 days of selection, the cells were cloned by limiting dilution, and one cell line (designated RAW-TT10) that showed good tetracycline-regulated expression from a subsequently transfected reporter plasmid was used for all experiments. Tetracycline was always absent from the media, resulting in strong activity of the tetracycline-regulated promoter.

Immunofluorescence microscopy

RAW cells were processed for immunofluorescence microscopy as described[25]. Cells grown on glass coverslips were incubated for 5 min at 37 °C with zymosan (Molecular Probes), fixed and permeabilized, and nonspecific sites were blocked by incubation in blocking buffer (PBS, 10% calf serum, 0.1% ovalbumin and 5 mM sodium azide). HA-tagged TLR2 was detected using a mouse monoclonal antibody (HA.11, Babco) precleared against zymosan. Specific binding was detected with fluorescein-conjugated goat anti-mouse secondary antibody (Jackson Immunoresearch). After mounting, the cells were observed by fluorescence microscopy using an Axiovert TV microscope (Carl Zeiss) equipped with a cooled CCD camera (Princeton Instruments) and Metamorph imaging software (Universal Imaging).

Luciferase assays

CHO-K1 cells were transiently transfected with 2 μg of NF-κB reporter construct (ELAM-1 firefly luciferase[26]) and 0.2 μg of a construct directing expression of *Renilla* luciferase under control of the constitutively active β-actin promoter[27], together with 3 μg of each of the expression constructs indicated in the text, and plated into 24-well tissue-culture plates. Twenty-four hours after transfection, the cells were stimulated with 3×10^6 zymosan particles (Molecular Probes) per well for 5 h, and luciferase activity was measured using the Dual-Luciferase Reporter Assay System (Promega) according to the manufacturer's instructions. Data are presented as the mean ± standard deviation of triplicate samples and are representative of three independent experiments.

Detection of intracellular TNF-α

S. aureus (clinical isolate) and *S. minnesota* (ATCC#49284) were grown to saturation, heat killed and stored as frozen aliquots. For particle stimulation, the RAW cells were incubated for 30 min at 37 °C with 3×10^6 zymosan (Molecular Probes), *S. aureus* or *S. minnesota* particles per well. After exposure to the particles, the cells were incubated for 4 h at 37 °C in the presence of 5 μg ml^{-1} brefeldin A to accumulate intracellular TNF-α. Where indicated, cells were exposed to 10 ng ml^{-1} LPS (*S. minnesota* R595, List), 10 μg ml^{-1} lipoteichoic acid (*S. aureus*, Sigma) or 10 μg ml^{-1} peptidoglycan (*S. aureus*, Fluka) with 5 μg ml^{-1} brefeldin A for 4 h at 37 °C. After blocking Fc-receptors with 2.4G2 hybridoma supernatant, the cells were fixed with 4% paraformaldehyde in PBS. The cells were permeabilized and stained with phycoerythrin-conjugated anti-mouse TNF-α (Pharmingen) diluted in 1% fetal calf serum and 0.1% saponin in PBS. After two washes, the cells were analysed by flow cytometry using a FACScan (Beckton Dickinson) and WinMDI software (Joseph Trotter, Scripps). Brefeldin A alone did not stimulate TNF-α production (data not shown).

Phagocytosis assay

Phagocytosis by RAW cells was measured by flow cytometry of cells that had ingested fluorescently labelled particles[25]. Zymosan, *S. aureus* or *S. minnesota* particles (3×10^6) labelled with tetramethylrhodamine were added to the macrophage monolayers and settled onto the cells by centrifugation. The cells were allowed to internalize the particles for 10 min at 37 °C, and uninternalized particles were washed away with PBS. For cells ingesting zymosan, remaining extracellular particles were dissolved by addition of 100 U ml^{-1} lyticase (Sigma) in PBS for 10 min at room temperature. The cells were resuspended in PBS + 1 mM EDTA, fixed in 1% formaldehyde, and analysed by flow cytometry. For cells ingesting bacteria, uninternalized bacteria were stripped from the cell surface by incubation in trypsin/EDTA for 5 min at room temperature, and the cells were fixed and analysed as above. It was confirmed by microscopy that the only remaining cell-associated fluorescently labelled particles had been internalized.

Received 19 August; accepted 10 September 1999.

1. Aderem, A. & Underhill, D. M. Mechanisms of phagocytosis in macrophages. *Annu. Rev. Immunol.* **17,** 593–623 (1999).
2. Medzhitov, R. & Janeway, C. A. Jr Self-defence: the fruit fly style. *Proc. Natl Acad. Sci. USA* **95,** 429–430 (1998).
3. Hoffmann, J. A., Kafatos, F. C., Janeway, C. A. & Ezekowitz, R. A. Phylogenetic perspectives in innate immunity. *Science* **284,** 1313–1318 (1999).
4. Lemaitre, B., Reichhart, J. M. & Hoffmann, J. A. *Drosophila* host defense: differential induction of antimicrobial peptide genes after infection by various classes of microorganisms. *Proc. Natl Acad. Sci. USA* **94,** 14614–14619 (1997).
5. Eldon, E. *et al.* The *Drosophila* 18 wheeler is required for morphogenesis and has striking similarities to Toll. *Development* **120,** 885–899 (1994).
6. Williams, M. J., Rodriguez, A., Kimbrell, D. A. & Eldon, E. D. The 18-wheeler mutation reveals complex antibacterial gene regulation in *Drosophila* host defense. *EMBO J.* **16,** 6120–6130 (1997).
7. Chaudhary, P. M. *et al.* Cloning and characterization of two Toll/Interleukin-1 receptor-like genes TIL3 and TIL4: evidence for a multi-gene receptor family in humans. *Blood* **91,** 4020–4027 (1998).
8. Rock, F. L., Hardiman, G., Timans, J. C., Kastelein, R. A. & Bazan, J. F. A family of human receptors structurally related to *Drosophila* Toll. *Proc. Natl Acad. Sci. USA* **95,** 588–593 (1998).
9. Takeuchi, O. *et al.* TLR6: a novel member of an expanding Toll-like receptor family. *Gene* **231,** 59–65 (1999).
10. Poltorak, A *et al.* Defective LPS signaling in C3H/HeJ and C57BL/10ScCr mice: mutations in TIr4 gene. *Science* **282,** 2085–2088 (1998).
11. Qureshi, S. T. *et al.* Endotoxin-tolerant mice have mutations in toll-like receptor 4 (Tlr4). *J. Exp. Med.* **189,** 615–625 (1999).
12. Stahl, P. D. & Ezekowitz, R. A. The mannose receptor is a pattern recognition receptor involved in host defense. *Curr. Opin. Immunol.* **10,** 50–55 (1998).
13. Hoshino, K. *et al.* Cutting edge: toll-like receptor 4 (TLR4)-deficient mice are hyporesponsive to lipopolysaccharide: evidence for TLR4 as the Lps gene product. *J. Immunol.* **162,** 3749–3752 (1999).
14. Heine, H. *et al.* Cutting edge: cells that carry A null allele for toll-like receptor 2 are capable of responding to endotoxin. *J. Immunol.* **162,** 6971–6975 (1999).
15. Yoshimura, A. *et al.* Cutting edge: recognition of Gram-positive bacterial cell wall components by the innate immune system occurs via toll-like receptor 2. *J. Immunol.* **163,** 1–5 (1999).
16. Schwandner, R., Dziarski, R., Wesche, H., Rothe, M. & Kirschning, C. J. Peptidoglycan- and lipoteichoic acid-induced cell activation is mediated by toll-like receptor 2. *J. Biol. Chem.* **274,** 17406–17409 (1999).
17. Medzhitov, R. *et al.* MyD88 is an adaptor protein in the hToll/IL-1 receptor family signaling pathways. *Mol. Cell.* **2,** 253–258 (1998).
18. Muzio, M., Ni, J., Feng, P. & Dixit, V. M. IRAK (Pelle) family member IRAK-2 and MyD88 as proximal mediators of IL-1 signalling. *Science* **278,** 1612–1615 (1997).
19. Wesche, H., Henzel, W. J., Schillinglaw, W., Li, S. & Cao, Z. MyD88: an adapter that recruits IRAK to the IL-1 receptor complex. *Immunity* **7,** 837–847 (1997).
20. Adachi, O. *et al.* Targeted disruption of the MyD88 gene results in loss of IL-1- and IL-18-mediated function. *Immunity* **9,** 143–150 (1998).
21. Freudenberg, M. A. & Galanos, C. Tumor necrosis factor α mediates lethal activity of killed gram-negative and gram-positive bacteria in D-galactosamine-treated mice. *Infect. Immun.* **59,** 2110–2115 (1991).
22. Kirschning, C. J., Wesche, H., Merrill Ayres, T. & Rothe, M. Human toll-like receptor 2 confers responsiveness to bacterial lipopolysaccharide. *J. Exp. Med.* **188,** 2091–2097 (1998).
23. Yang, R. B. *et al.* Toll-like receptor-2 mediates lipopolysaccharide-induced cellular signalling. *Nature* **395,** 284–288 (1998).
24. Gossen, M. & Bujard, H. Tight control of gene expression in mammalian cells by tetracycline-responsive promoters. *Proc. Natl Acad. Sci. USA* **89,** 5547–5551 (1992).
25. Underhill, D. M., Chen, J., Allen, L. A. & Aderem, A. MacMARCKS is not essential for phagocytosis in macrophages. *J. Biol. Chem.* **273,** 33619–33623 (1998).
26. Schindler, U. & Baichwal, V. R. Three NF-κB binding sites in the human E-selectin gene required for maximal tumor necrosis factor α-induced expression. *Mol. Cell. Biol.* **14,** 5820–5831 (1994).
27. Sweetser, M. T. *et al.* The roles of nuclear factor of activated T cells and ying-yang 1 in activation-induced expression of the interferon-γ promoter in T cells. *J. Biol. Chem.* **273,** 34775–34783 (1998).

Supplementary information is available in *Nature*'s World-Wide Web site (http://www.nature.com) or as paper copy from the London editorial office of *Nature*.

Acknowledgements

Supported in part by grants from the NIH (A.A., C.B.W. and A.S.) and from the cystic fibrosis foundation (C.B.W. and A.H.). D.M.U. is an Irvington Institute postdoctoral fellow.

Correspondence and requests for materials should be addressed to A.A. (e-mail: aaderem@u.washington.edu).

Table 1 Bone mineral density

Groups	BMD in metaphysis (mg cm^{-3})		BMD in diaphysis (mg cm^{-3})	
	Total	Trabecular	Total	Trabecular
rag1$^{-/-}$	363.3 ± 14.5	309.5 ± 18.5	644.4 ± 3.6	ND
ctla4$^{+/-}$*rag1*$^{-/-}$	379.6 ± 7.3	291.5 ± 15.6	626.4 ± 17.0	462.8 ± 19.6
ctla4$^{-/-}$*rag1*$^{-/-}$	302.7 ± 14.9*	209.5 ± 44.9*	529.8 ± 3.4*	353.0 ± 10.8*

Bone mineral density (BMD) was measured by peripheral quantitative computated tomography of tibial bones from *rag1*$^{-/-}$ ($n = 3$) and *rag1*$^{-/-}$ mice reconstituted with *ctla4*$^{+/-}$ ($n = 3$) or *ctla4*$^{-/-}$ ($n = 3$) bone marrow cells eight weeks after cell transfer.
* Statistically significant difference between different groups (Student's *t*-test: $P < 0.05$). Values are given as the mean ± s.d. ND, not determined.

Nature **402**, 304–309; 1999

Activated T cells regulate bone loss and joint destruction in adjuvant arthritis through osteoprotegerin ligand

Young-Yun Kong*†, Ulrich Feige†‡, Iidiko Sarosi§, Brad Bolon§, Anna Tafuri*, Sean Morony§, Casey Capparelli§, Ji Li‖, Robin Elliott‖, Susan McCabe‖, Thomas Wong¶, Giuseppe Campagnuolo‡, Erika Moran#, Earl R. Bogoch#, Gwyneth Van§, Linh T. Nguyen☆, Pamela S. Ohashi☆, David L. Lacey§, Eleanor Fish¶, William J. Boyle‖ & Josef M. Penninger*☆

** Amgen Institute, 620 University Avenue, Toronto, Ontario M5G 2C1, Canada*
‡ Department of Pharmacology, § Pathology, and ‖ Cell Biology, Amgen Inc., One Amgen Center Drive, Thousand Oaks, California 91320-1789, USA
¶ Department of Medical Genetics & Microbiology, # St Michael's Hospital
☆ Ontario Cancer Institute and the Departments of Medical Biophysics and Immunology, University of Toronto, Toronto, Ontario, Canada
† These authors contributed equally to this work

Bone remodelling and bone loss are controlled by a balance between the tumour necrosis factor family molecule osteoprotegerin ligand (OPGL) and its decoy receptor osteoprotegerin (OPG)[1–3]. In addition, OPGL regulates lymph node organogenesis, lymphocyte development and interactions between T cells and dendritic cells in the immune system[3–5]. The OPGL receptor, RANK, is expressed on chondrocytes, osteoclast precursors and mature osteoclasts[4,6]. OPGL expression in T cells is induced by antigen receptor engagement[7], which suggests that activated T cells may influence bone metabolism through OPGL and RANK. Here we report that activated T cells can directly trigger osteoclastogenesis through OPGL. Systemic activation of T cells *in vivo* leads to an OPGL-mediated increase in osteoclastogenesis and bone loss. In a T-cell-dependent model of rat adjuvant arthritis characterized by severe joint inflammation, bone and cartilage destruction and crippling, blocking of OPGL through osteoprotegerin treatment at the onset of disease prevents bone and cartilage destruction but not inflammation. These results show that both systemic and local T-cell activation can lead to OPGL production and subsequent bone loss, and they provide a novel paradigm for T cells as regulators of bone physiology.

Remodelling of bone involves the synthesis of bone matrix by osteoblasts and bone resorption by osteoclasts[8]. Excessive osteoclast activity is observed in many osteopenic disorders characterized by increased bone resorption and crippling bone damage, including post-menopausal osteoporosis[9], Paget's disease[10] and lytic bone metastases[11]. Local or generalized bone loss has also been reported in chronic infections (hepatitis, HIV)[12], leukaemias[13], autoimmune and allergic diseases[14], and rheumatoid arthritis[15], suggesting that an activated immune system can affect bone physiology. Although cytokines, such as tumour necrosis factor (TNF)α, interleukin (IL)-1, IL-11 and IL-17[16], that regulate immune functions have been implicated in the regulation of bone homeostasis, the molecular mechanism by which the immune system affects bone metabolism has never been established.

Consistent with previous reports[7,17], we observed that OPGL (also known as TRANCE, RANK-L or ODF) messenger RNA expression was upregulated in murine T cells following antigen receptor engagement (Fig. 1a). Specific inhibitor studies showed that induction of OPGL was dependent on protein kinase C (PKC), phosphoinositide 3-kinase (PI3K) and calcineurin-mediated signalling pathways (Fig. 1a). Expression of OPGL protein was detected on the surfaces of activated, but not resting, T cells (Fig. 1b). Activated T cells also secreted soluble OPGL into culture medium (Fig. 1c), and soluble OPGL was detected by enzyme-linked immunosorbent assay (ELISA) (~2.2 ± 0.2 ng ml^{-1} of OPGL in the culture supernatant of CD4$^+$ T cells activated for 4 days with αCD3 plus αCD28). To determine whether the secreted and/or surface forms of OPGL were functionally active, we assessed the ability of both molecules to induce osteoclastogenesis *in vitro*. Haematopoietic bone marrow precursors from wild-type mice were co-cultured with activated CD4$^+$ T cells fixed with paraformaldehyde or with culture supernatants from activated T cells. Both membrane-bound and soluble OPGL supported osteoclast development *in vitro* (Fig. 1d). Osteoclastogenesis was blocked in both cases in the presence of the physiological decoy receptor osteoprotegerin (OPG) (Fig. 1d). As certain T-cell-derived cytokines can regulate OPGL expression in stromal cells, we neutralized many different cytokines including IL-1, TNFα, IL-6, interferon (INF)γ, IL-3, and granulocyte/macrophage colony-stimulating factor (GM-CSF), and none of these cytokines proved critical for *in vitro* osteoclastogenesis in this culture system, confirming that T-cell-derived OPGL is the crucial mediator. To exclude the possibility that another surface receptor on fixed T cells activates stromal cells for OPGL expression, we used spleen cells from newborn *opgl*$^{-/-}$ mice as a source of haematopoietic precursors and fixed wild-type CD4$^+$ T cells. In this culture, the only source of OPGL is membrane-bound OPGL on the T cells. Wild-type T cells induced the formation of tartrate-resistant acid phosphatase (TRAP)$^+$ osteoclasts from *opgl*$^{-/-}$ progenitor cells, and osteoclastogenesis was inhibited by addition of OPG (Fig. 1d). Osteoclastogenesis was confirmed by detection of the osteoclast-specific markers calcitonin receptor (CTR), RANK (Fig. 1e), cathepsin K (Fig. 1f) and β_3-integrin (Fig. 1g). Thus, T-cell-triggered osteoclasts display a typical osteoclast phenotype (TRAP$^+$, CTR$^+$, cathepsin K$^+$, β_3-integrin$^+$, RANK$^+$). These results provide genetic evidence that activated T cells can directly trigger osteoclastogenesis through membrane-bound and soluble OPGL.

To evaluate whether T-cell activation and expression of OPGL affect bone physiology *in vivo*, we explored the phenotype of *ctla4*$^{-/-}$ mice, in which T cells are spontaneously activated[18]. All *ctla4*$^{-/-}$ mice displayed severe osteoporosis compared with heterozygote littermates (Fig. 2a–d). To further explore the effect of spontaneously activated T cells on bone metabolism, we adoptively transferred *ctla4*$^{+/-}$ or *ctla4*$^{-/-}$ bone marrow cells into lymphocyte-deficient